Thermal-noise-limited optical cavity

S. A. Webster,[1] M. Oxborrow,[1] S. Pugla,[2] J. Millo,[3] and P. Gill[1]
[1]*National Physical Laboratory, Hampton Road, Teddington, Middlesex, TW11 0LW, United Kingdom*
[2]*Blackett Laboratory, Imperial College London, South Kensington Campus, London, SW7 2BZ, United Kingdom*
[3]*SYRTE, Observatoire de Paris, 61, Avenue de l'Observatoire, 75014, Paris, France*
(Received 31 October 2007; published 27 March 2008)

A pair of optical cavities are designed and set up so as to be insensitive to both temperature fluctuations and mechanical vibrations. With the influence of these perturbations removed, a fundamental limit to the frequency stability of the optical cavity is revealed. The stability of a laser locked to the cavity reaches a floor $<2\times10^{-15}$ for averaging times in the range 0.5–100 s. This limit is attributed to Brownian motion of the mirror substrates and coatings.

DOI: 10.1103/PhysRevA.77.033847 PACS number(s): 42.60.Da, 07.60.Ly, 07.10.Fq, 06.30.Ft

I. INTRODUCTION

Frequency-stable lasers are essential to the operation of optical atomic frequency standards. The precision with which an atomic transition is resolved depends on the spectral width of the laser used to interrogate it. This is true down to the level where one resolves the natural linewidth of the transition, which for many of the systems under investigation, is around the Hz level. However, where it is ~mHz [1] or even ~nHz [2], the atomic linewidth can, in effect, be considered to be a δ function and the observed Q is determined purely by the laser source. Thus the motivation exists for striving toward the limits of laser linewidth and stability.

At the heart of a stable laser system is an optical cavity, usually taking the form of a nonconfocal Fabry-Pérot etalon: two highly reflective curved mirrors optically contacted to a cylindrical spacer with an axial bore hole. The laser's frequency is stabilized to a longitudinal mode of the cavity and, given a sufficiently high fidelity of control to this mode, the frequency is defined by the length of the cavity. The requirement for frequency stability thus translates into requiring that the cavity's optical length, as defined by its spacer and mirrors, be dimensionally stable. Needless to say, achieving the lowest level of frequency instability presents a considerable technical challenge. For a cavity of length 0.1 m, perturbations in length ~1 fm correspond to frequency changes ~1 Hz and these may arise in various ways. Temperature changes couple to length through thermal expansion and vibrations, entering through supports, cause the cavity to deform. However, by exploiting material properties and through careful engineering of the cavity's form, one can overcome these sources of technical noise.

Having suppressed perturbations of a technical origin, one then reveals a more fundamental source of noise: Brownian motion, due to local thermal fluctuations in the mirror substrates and coatings, giving rise to length fluctuations. The role of thermal fluctuations in limiting the frequency stability of rigid, laboratory-based cavities has been proposed by Numata *et al.* [3] following earlier work to characterize this effect in relation to gravitational wave detectors [4]. Their calculation of the thermal noise in the cavity used to achieve the best frequency stability to date [5] corresponds well with experimental observations and they conclude that the measured stability is seemingly limited by thermal noise. A subsequent experiment has investigated these predictions [6] for a variety of materials and geometries and has also found the experimental results to be comparable to the theoretical model. More recently, thermal-noise-limited behavior has been observed in another experiment where light is locked to a cavity with a frequency stability at the part in 10^{15} level [7].

This paper follows up Ref. [8] which describes a vibration insensitive design and experimentally demonstrates a null in the response to vertical acceleration. In this work, we present the critical test of the technique: a measurement of the relative frequency stability of two cavities made to the vibration insensitive design. The first section of the paper describes a design of temperature control in which Peltier cooling internal to the vacuum chamber allows the cavity to be cooled to $-10\,^{\circ}\mathrm{C}$, well below the temperature of zero expansivity. This leads to a clear observation of a turning point in the cavity's frequency as a function of temperature and, with the aid of thermal modeling, a determination of the temperature at which the coefficient of thermal expansion goes to zero. The second section reiterates the vibration-insensitive design and presents data for the acceleration response of the two cavities used in this work. The finite element analysis described in the previous paper is validated by an independent model. The quantitative agreement between the models and the experimental data is a factor of 3 better than was previously shown.

With both cavities temperature controlled at their zero in expansivity and made insensitive to vibrations, the final section describes the experiment performed to measure the relative frequency fluctuations between light locked to the two cavities. The contributions of vibrations to the frequency noise and of temperature to the long term frequency drift are shown to be negligible. We report a frequency stability of $<2\times10^{-15}$ for an averaging time τ in the range 0.5–100 s. Further, with frequency drift canceled to second order, the fractional stability remains below 3×10^{-15} out to 1000 s. This is the lowest stability to have been reported for an optical oscillator at this time scale. For $0.5<\tau<500$ s, the Allan deviation is proportional to $\tau^{0.07}$, in good qualitative agreement with the theoretical model for thermal noise which predicts a τ^{0} dependence. The quantitative agreement with theory is also good considering the remaining uncer-

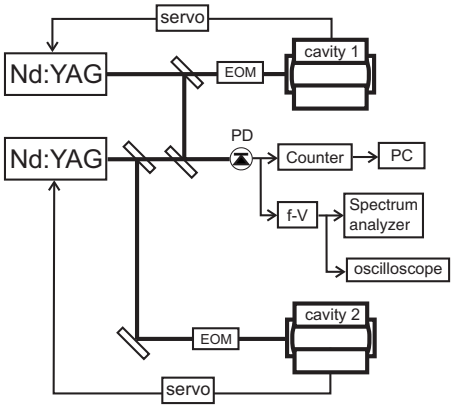

FIG. 1. Experimental scheme for measuring the frequency difference between two cavities. PD, photodiode; EOM, electro-optic modulator. The thicker lines indicate beam paths; the thinner lines indicate electronic signal paths.

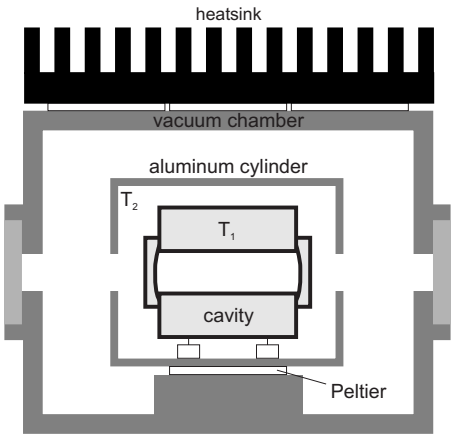

FIG. 2. Vacuum housing for cavity with two-stage temperature control. The vacuum chamber is cooled and controlled at 15 °C using Peltier heat pumps. The internal aluminum cylinder is cooled further, to a temperature T_2 using a single Peltier element, and, with this, it is possible to cool to −10 °C.

tainties in the model. Thus, this work provides confirmation of the surprising and important observation: that Brownian motion in the mirror substrates and coatings is limiting the frequency stability of rigid optical cavities.

II. THERMAL EXPANSIVITY

The cavities used in this work are made entirely from ultra-low-expansivity glass (ULE) which nominally has a zero in its thermal expansivity at room temperature (≈25 °C). However, experience shows that often the zero occurs below room temperature [9]. An experiment is conducted to locate the temperature of the zero crossing for the two cavities. A Nd:YAG laser is locked to each cavity and a beat note between the two lasers detected. The scheme is shown in Fig. 1. Further details of the locking scheme may be found in Ref. [10]. One cavity is temperature controlled, while the other is first cooled and then heated. On passing through zero, the expansivity changes sign and the beat frequency goes through a turning point. By simultaneously monitoring the frequency and temperature, one can then determine the temperature at which the zero crossing occurs.

Two vacuum chambers are set up to allow the cavities to be cooled. The design is shown in Fig. 2. The cavity is situated within an aluminum cylinder, cooled and temperature controlled by a Peltier element. The temperature is measured and independently monitored by thermistors in bridge circuits. The chamber is also cooled by Peltier elements and is controlled at 15 °C. As the cylinder and cavity are within vacuum, the temperature can be decreased below the dew point without risk of condensation on optics and with this apparatus it is possible to cool down to −10 °C. Initially, the cavity is cooled over the period of a day to a temperature well below that expected for the zero-crossing temperature. Heating is achieved simply by disconnecting the temperature control and allowing the cavity to return to room temperature.

The cavity's temperature is not measured directly, but is inferred from the temperature of the surrounding aluminum cylinder using a simple thermal model. It is assumed throughout that the temperatures of both the cavity and aluminum cylinder are sufficiently uniform for them to be respectively described by the single variables T_1 and T_2. Assuming changes in the temperature are relatively small, one can approximate the rate of change of T_1 as

$$\frac{dT_1[t]}{dt} = c(T_2[t] - T_1[t]), \tag{1}$$

where c is a constant dependent upon the various geometrical and physical properties of the cavity and cylinder. Multiplying the equation by e^{ct} on both sides and integrating between the limits $-\infty$ and τ, one obtains the following solution for T_1 in terms of T_2 as a function of time:

$$T_1[\tau] = c\int_{-\infty}^{\tau} e^{c(t-\tau)}T_2[t]dt. \tag{2}$$

Assuming that $dT_2/dt=0$ for $-\infty<t<0$, the solution can be further simplified to

$$T_1[\tau] = T_2[0]e^{-c\tau} + c\int_{0}^{\tau} e^{c(t-\tau)}T_2[t]dt. \tag{3}$$

An initial guess is made for c and $T_1[\tau]$ is calculated using Eq. (3). Frequency, also known as a function of time, is then plotted against T_1 for both the heating and cooling data. It is reasonable to assume that the temperature of the zero in expansivity is the same whether one is heating or cooling the cavity. Therefore, the correct value of c is that which makes the turning points for the heating and cooling data coincide. The value of c is iterated until as close an overlap as possible of the heating and cooling curves is achieved, at which point the temperature scale T_1 is determined.

Figures 3(a) and 3(b) show the heating and cooling data for the two cavities. The turning point occurs at a temperature of 9.2 °C for cavity 1 and 8.3 °C for cavity 2. The overlap between the heating and cooling curves is not perfect due to the approximations made in the model used to derived

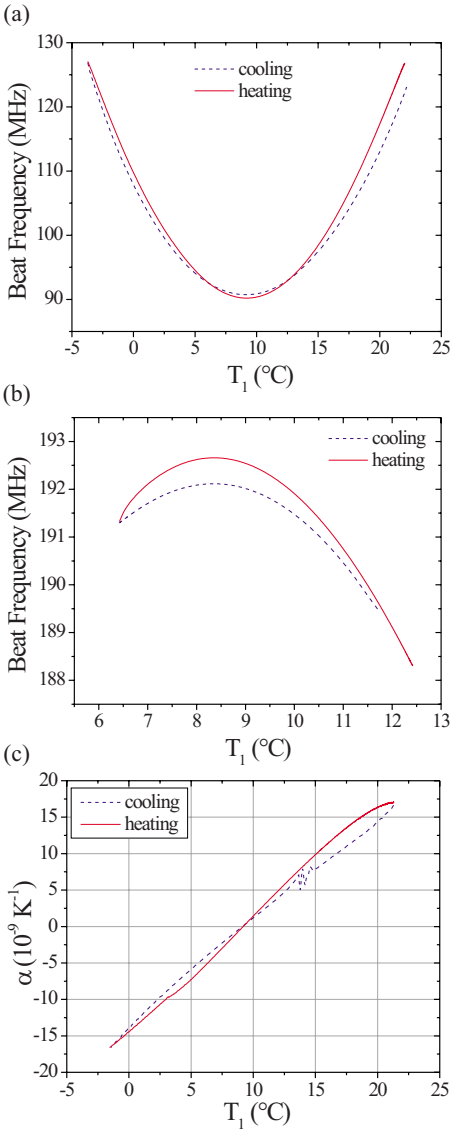

FIG. 3. (Color online) Plot of beat frequency as a function of cavity temperature for (a) cavity 1 and (b) cavity 2. (c) Thermal expansivity as a function of cavity temperature, derived from the data for cavity 1.

the temperature scale. In particular, no allowance has been made for the presence of thermal gradients within the cavity itself which is assumed to have a uniform temperature. Figure 3(c) shows the thermal expansivity of cavity 1 as a function of temperature, obtained by taking the derivative of the frequency data. The rate of variation of α with temperature about the zero crossing is 1.5×10^{-9} K^{-2}.

III. VIBRATION INSENSITIVITY

The two cavities are modified so as to be vibration insensitive, according to the design outlined in Ref. [8]. Square "cutouts" are made to the underside of the cavity's cylindrical spacer and, for a certain separation of the support points, the response to vertical vibrations is nulled. Further, symmetry in the supports, both in the geometry and in the restoring

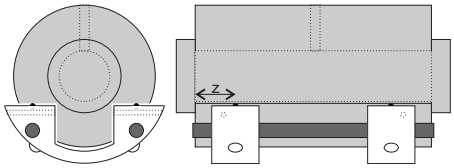

FIG. 4. Cutout cavity on mount. The cavity is supported at four points on 3 mm diameter rubber spheres which are located within "yokes," shown in white.

forces acting at the contact points, ensures a null in the horizontal response. The cavity on its mount is shown in Fig. 4. This is then placed within the aluminum cylinder inside the vacuum chamber shown in Fig. 2. The position of the supports may be varied by sliding the yokes (see the caption of Fig. 4) along the parallel rods.

"Shake testing" is performed to locate the vertical response null for both cavities. As before, a Nd:YAG laser is locked to each cavity and a beat note between the two lasers detected. Both cavities are situated on active vibration isolation platforms, and while the isolation is engaged for one cavity, the second is operated in reverse as a "shaker." A sinusoidal acceleration at 15 Hz is applied and the response of the cavity detected as modulation of the beat note. The modulation frequency is low enough that the response may be considered to be quasistatic and is below any resonances in the support structure. Acceleration is measured using a three-axis seismometer and the amplitude of frequency modulation on the beat is measured on a spectrum analyzer following frequency-to-voltage conversion. The sign of the response is also noted by viewing the beat and seismometer output directly on an oscilloscope. This measurement is repeated for several positions of the support until a satisfactory null in the vertical response is found. With each iteration, the cavity is removed from the vacuum chamber, the support position changed, the cavity and mount replaced within the vacuum chamber, and the vacuum pumped down to a pressure ~1 mbar.

Figure 5 shows the results of the shake test. The vertical response null occurs for $z_0=16.5$ (15.8) mm and the sensitivity to the support position is 3.6 (3.5) kHz/ms^{-2} per mm

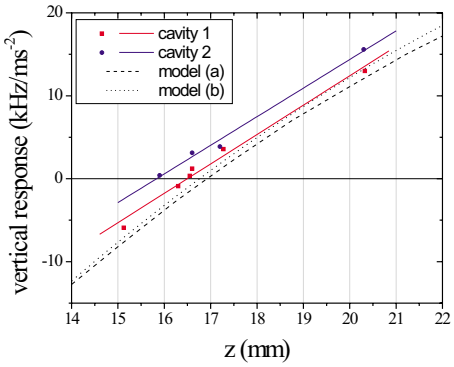

FIG. 5. (Color online) Plot showing the response to vertical acceleration. The straight lines are linear fits to the data. The results of finite-element models of the vertical response developed at (a) NPL and (b) SYRTE, are also shown.

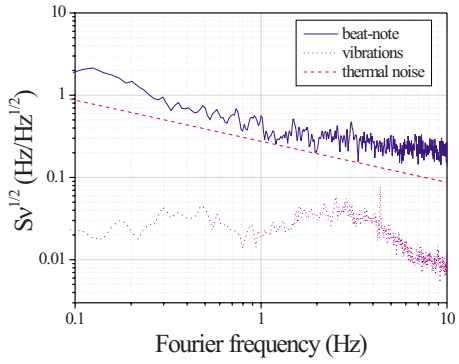

FIG. 6. (Color online) Plot of root spectral power density of frequency fluctuations of the beat signal as a function of Fourier frequency. Also shown are the predicted contribution to the frequency noise from vibrations and a calculation of the thermal noise.

in z for cavity 1 (cavity 2). The figure also shows the results of two finite element analyses: the model introduced in the previous work [8] and a model developed independently at SYRTE using a different software package [11]. The quantitative agreement between the models is good: the x intercepts agree to within 1% and the slopes agree to within 3%, thus giving validity to the model developed by the National Physical Laboratory (NPL). Previously, there was some quantitative discrepancy between the experimental data and the model: the x intercept differed by 20% and the slope differed by a factor of 2, and the reason for this is still unknown. Here the correspondence between the models and both data sets is much better. The x intercepts of the data differ from the NPL model by 3% (6%) and the slopes differ by 12% (14%) for cavity 1 (cavity 2). The amplitude of the horizontal response varies in the range $1-10$ kHz/ms^{-2}. This is due to residual asymmetry in the supports and the variation is an indication of the reproducibility of the placement of the cavity on the mount with each iteration in z. Once a satisfactory vertical response null is located for each cavity, the vacuum chambers are pumped down to a pressure ($\sim 10^{-7}$ mbar) and the vibration response tested once more. The final values obtained for the vertical, north, east vibration response are $(0.84, 3.6, 4.7)$ kHz/ms^{-2} and $(0.45, 3.3, 0.96)$ kHz/ms^{-2} for cavities 1 and 2, respectively, where north (east) correspond to horizontal directions along (perpendicular to) the optical axis.

IV. THERMAL-NOISE LIMIT

With the two cavities controlled at their zero in thermal expansivity and setup for minimum vibration response, an experiment is conducted to measure the relative frequency noise between light locked to the two cavities. The beat note is analyzed by converting it to a voltage and then measuring the spectrum of frequency fluctuations. Figure 6 shows the result. In addition to the spectral power density of the optical signal, the plot shows the contribution to the frequency noise from vibrations and a calculation of the thermal noise. The frequency noise due to vibrations is derived from a measurement of the ambient acceleration on the isolation platforms and the measured three-dimensional vibration response of both cavities. The thermal noise is calculated following the approach of Numata *et al.* [3]. The contribution from one end of the spacer is $\sqrt{S}_{\text{spacer}}=2.7\times10^{-18}f^{-1/2}$ m and the contribution from each mirror substrate is $\sqrt{S}_{\text{substrate}}=3.92\times10^{-17}f^{-1/2}$ m, where the temperature is 285 K, the length of the cavity is 0.1 m, the radius of the spacer is 0.3 m, the beam radius at the mirror is 220 μm, and Young's modulus, the Poisson ratio, and the mechanical loss coefficient of ULE are taken to be 67.6 GPa, 0.17, and $1/6\times10^{4}$, respectively. An additional loss is introduced by the mirror coating, and taking account of this, the contribution from each mirror is $\sqrt{S}_{\text{mirror}}=4.83\times10^{-17}f^{-1/2}$ m, where the mirror coating is 5.3-μm thick [12] and the mechanical loss coefficient of the coating is taken to be 4×10^{-4}. Summing the contributions from both ends of the spacer and both mirrors in quadrature, gives a total displacement noise for one cavity of $\sqrt{S}_{\text{cavity}}=6.84\times10^{-17}f^{-1/2}$ m. The frequency noise arising from these displacement fluctuations is $\sqrt{S}_{\nu}=0.193f^{-1/2}$ Hz, where the wavelength of light used is 1064 nm. The data are a measure of the relative frequency fluctuations between two nominally identical cavities. Therefore, the measured relative frequency noise is predicted to be $\sqrt{S}_{\nu}=0.27f^{-1/2}$ Hz.

One can see from Fig. 6 that, apart from one peak around 4 Hz, the frequency noise due to vibrations is at least an order of magnitude lower than the measured level. Thus, one can say that, in this setup, perturbations due to vibrations have effectively been eliminated. In the range $0.3-3$ Hz, the frequency noise has a slope of $1/\sqrt{f}$, characteristic of thermal noise and, given the remaining uncertainties in the model, such as the exact values of the mechanical loss coefficients at the frequencies of interest here, the quantitative agreement is also reasonable. The deviation of the data from the $1/\sqrt{f}$ slope may be attributed to measurement noise at high frequency (>3 Hz) and drift at low frequency (<0.3 Hz). Even with drift compensation, the discrepancy remains at low frequency, and the additional noise is thought to be due to the influence of air currents in the beam path through the presence of weak "parasitic" etalons coupled to the high finesse cavity.

Evidence of parasitic etalons is seen in this experimental setup. Normally, the optical bench is enclosed, but on removing the covers the frequency noise in the range $0.1-1$ Hz is observed to rise by around a factor of 4. Further, if one deliberately disturbs the air above the beam path, the frequency of the beat fluctuates by as much as 10 Hz. One consideration in trying to minimize the effect of parasitic etalons is the choice of modulation frequency. The accuracy of the frequency lock depends, very sensitively, on the detection of the relative phase of the carrier and sidebands in the reflected field from the high-finesse cavity. Where a parasitic etalon is present, this phase becomes dependent on the optical path length between the high-finesse cavity and the back-reflecting (scattering) surface that is cause of the etalon. By reducing the separation in frequency between the carrier and sidebands, one reduces the sensitivity of the phase to changes in the optical path length. In the experimental setup shown in Fig. 1, light is frequency modulated by electro-optic modulators operating at frequencies close to 10 MHz. The modulation frequency may be significantly reduced

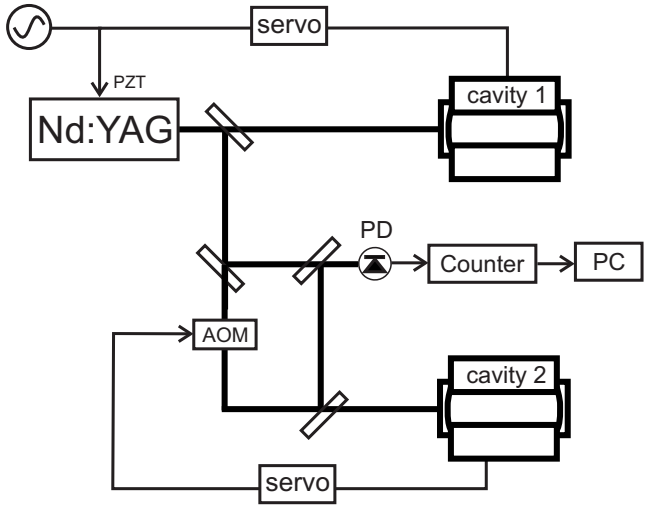

FIG. 7. Experimental scheme for measuring frequency difference between two cavities with piezoelectric frequency modulation. PD, photodiode; PZT, piezoelectric. The thicker lines indicate beam paths; the thinner lines indicate electronic signal paths.

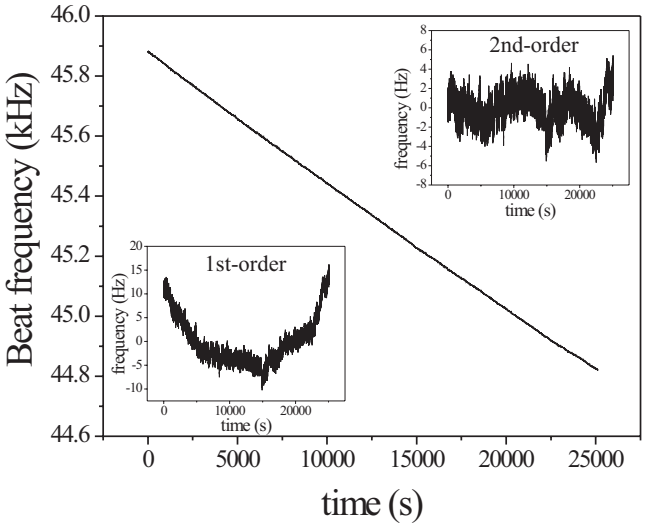

FIG. 8. Plot of beat frequency as a function of time. The insets are the residuals from first- and second-order polynomials fits to the data.

without detriment to the bandwidth of the frequency servo and the particular laser source used here, a nonplanar ring oscillator Nd:YAG, offers a simple and effective means of doing so. The laser's frequency is tuned by application of a voltage to a piezoelectric crystal bonded directly onto the laser crystal. There exist low-frequency piezoelectric resonances which allow one to impress strong frequency modulation sidebands onto the light without there being any measurable residual amplitude modulation. The experiment was therefore modified, replacing electro-optic modulation with piezoelectric modulation at a frequency of 337 kHz, corresponding to a resonance with a particularly low level residual amplitude modulation. The scheme is shown in Fig. 7. A consequence of directly modulating the laser frequency is that one no longer has access to an unmodulated beam. If required, an unmodulated beam could be obtained with this scheme by filtering the modulated light. One could use the transmission of the optical cavity to which the light is locked, or, alternatively, the transmission from a second tunable cavity locked to the frequency of the light. One could also continue with external electro-optic modulation at a lower frequency, however, this was not tested in this work.

The frequency of the beat note is measured once more and this time a record is taken over a period of several hours to determine the long-term behavior. This is done using a frequency counter connected to a PC, sampling once every second. Figure 8 shows the result. The frequency exhibits predominantly linear drift with a magnitude of 45 mHz/s. This rate is maintained to within ± 5 mHz/s over the long term and is attributed to isothermal "creep" of the ULE material from which the cavities are made. The lower (upper) inset to Fig. 8 shows the residuals from a first- (second-) order polynomial fit to the data. After removing the linear term, the residual drift, which may be temperature dependent, is two orders of magnitude smaller. Therefore, one can say that temperature fluctuations have to a large extent been eliminated. The fractional Allan deviation is calculated from the frequency record for averaging times in the range 2–4000 s and is shown in Fig. 9. For averaging times in the range 1 ms–10 s, the Allan deviation is calculated directly using the frequency counter's own internal algorithm. The predicted thermal noise is also shown on the plot. Where the spectral power density $\sqrt{S_\nu} \propto 1/\sqrt{f}$, the Allan deviation is independent of averaging time and is calculated to be $\sigma = \sqrt{S_\nu 2 \ln(2) f} = 1.15 \times 10^{-15}$, where $\sqrt{S_\nu}$ is taken to be the relative frequency noise between the cavities. Short time scales ($\tau = 1-200$ ms) exhibit $1/\sqrt{\tau}$ behavior or white frequency noise, but a limit of 1.5×10^{-15} is met at an averaging time of 0.5 s. Linear drift, having a slope proportional to τ, is observed for $\tau > 10$ s, but, with this taken out, σ/ν remains below 2×10^{-15} out to an averaging time of 100 s. Second-order drift is apparent for $\tau > 100$ s, and removing

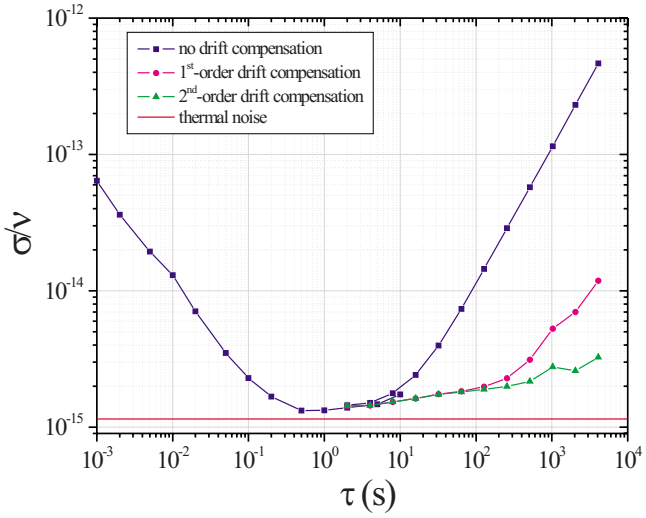

FIG. 9. (Color online) Plot of fractional Allan deviation as a function of sample time. A calculation of the thermal noise is also shown.

this σ/ν remains below 3×10^{-15} out to 1000 s. Having taken out drift, the Allan deviation of the residual frequency fluctuations is proportional to $\tau^{0.07}$. This is in good qualitative agreement with the theoretical model for thermal noise, which predicts a τ^0 dependence, and, again, considering the remaining uncertainties in the model, the quantitative agreement is also good. One may therefore attribute the observed behavior to thermal noise arising largely within the mirror substrates and their coatings.

V. CONCLUSION

We have demonstrated optical cavities that are insensitive to both temperature fluctuations and mechanical vibrations and this being the case, we have effectively eliminated the influence of these perturbations. A reduction of the modulation frequency used in the locking scheme has also reduced the influence of parasitic etalons, which couple in instability from air currents in the beam path. All this has revealed an underlying limit due to thermal noise. The frequency stability reaches a floor of $<2\times10^{-15}$ for averaging times in the range, 0.5–100 s, in agreement with the calculations of Numata *et al.* This confirms that thermal fluctuations are indeed the limitation to further reduction in laser linewidth.

ACKNOWLEDGMENTS

This work is supported by the NMS quantum metrology program under Contract No. FQM1/AO1.

[1] M. Takamoto and H. Katori, Phys. Rev. Lett. **91**, 223001 (2003).
[2] M. Roberts, P. Taylor, G. P. Barwood, P. Gill, H. A. Klein, and W. R. C. Rowley, Phys. Rev. Lett. **78**, 1876 (1997).
[3] K. Numata, A. Kemery, and J. Camp, Phys. Rev. Lett. **93**, 250602 (2004).
[4] K. Numata, M. Ando, K. Yamamoto, S. Otsuka, and K. Tsubono, Phys. Rev. Lett. **91**, 260602 (2003).
[5] B. C. Young, F. C. Cruz, W. M. Itano, and J. C. Bergquist, Phys. Rev. Lett. **82**, 3799 (1999).
[6] M. Notcutt, L-S. Ma, A. D. Ludlow, S. M. Foreman, J. Ye, and J. L. Hall, Phys. Rev. A **73**, 031804(R) (2006).
[7] A. D. Ludlow, X. Huang, M. Notcutt, T. Zanon-Willette, S. M. Foreman, M. M. Boyd, S. Blatt, and J. Ye, Opt. Lett. **32**, 641 (2007).
[8] S. A. Webster, M. Oxborrow, and P. Gill, Phys. Rev. A **75**, 011801(R) (2007).
[9] Other users of ULE in the field of optical frequency metrology (private communication).
[10] S. A. Webster, M. Oxborrow, and P. Gill, Opt. Lett. **29**, 1497 (2004).
[11] The modeling was carried out using CASTEM 2000.
[12] Ramin Lalezari, ATFilms (private communication).